Mechanistic Investigation of Rh(I)-Catalyzed Asymmetric Suzuki-Miyaura Coupling with Racemic Allyl Halides

Lucy van Dijk,[a]† Ruchuta Ardkhean,[a,b]† Mireia Sidera,[a,c]† Sedef Karabiyikoglu,[a] Özlem Sari,[a,d] Timothy D. W. Claridge,[a]* Robert S. Paton,[a,e]* and Stephen P. Fletcher[a]*

[a] Department of Chemistry, Chemistry Research Laboratory, University of Oxford, 12 Mansfield Road, Oxford, OX1 3TA, UK.

[b] Faculty of Medicine and Public Health, HRH Princess Chulabhorn College of Medical Science, Chulabhorn Royal Academy, Bangkok, Thailand.

[c] Vertex Pharmaceuticals (Europe) Ltd, 86-88 Jubilee Avenue, Milton Park, OX14 4RW, UK.

[d] Department of Chemistry, Middle East Technical University, 06800 Ankara, Turkey; Department of Chemistry, Kirsehir Ahi Evran University, 40100, Kirsehir, Turkey.

[e] Department of Chemistry, Colorado State University, Fort Collins, CO 80523, USA

† L.v.D, R.A and M.S. contributed equally to this work.

Abstract: A catalytic cycle is proposed for the highly enantioselective Rh(I)-catalyzed Suzuki-Miyaura coupling of boronic acids and racemic allyl halides based on a combination of experimental and computational studies. Natural abundance ^{13}C kinetic isotope effects are used to provide quantitative information about the transition state structures of two key elementary steps in the catalytic cycle – transmetalation and oxidative addition. Experiments using configurationally stable, deuterium labelled substrates reveal that oxidative addition can happen *via syn*- or *anti*-pathways. DFT calculations attribute the extremely high enantioselectivity to reductive elimination from a η^3 Rh complex formed from both allyl halide enantiomers. Our conclusions are supported by NMR spectroscopic studies and competition experiments. This study provides unparalleled insight into the sequence of bond-forming steps of the titular reaction and their transition state structures. This will contribute to the broader understanding of Rh-allyl chemistry and enable the discovery of asymmetric reactions with racemic substrates.

Suzuki-Miyaura cross-coupling is used extensively for Csp^2–Csp^2 bond formation (Fig. 1a). One reason for the broad adaptation of this method is the wide range of organoboron reagents that are readily available and easy to handle, providing advantages over other organometallic reagents.[1] Since the first report in 1979, tremendous effort has been directed towards further development, leading to Suzuki's receipt of the 2010 Nobel Prize in Chemistry alongside Heck and Negishi.[2]

The development of asymmetric cross-coupling transformations with organoboron reagents is an area of active investigation. Reported strategies include starting from single enantiomer alkylboronates, enantiopure

electrophiles, and desymmetrizations.[3] Boronic acids and derivatives have been employed in enantioselective allylic arylations mostly catalyzed by Rh,[4, 5] Cu,[6] Pd[7] and Ni.[8] Some stereospecific allylic arylations have also been developed using Pd[9] and Cu.[10]

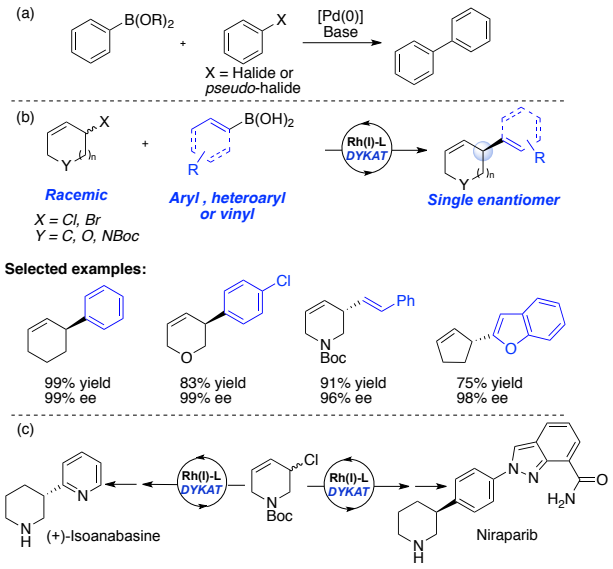

Figure 1. (a) Classical Suzuki-Miyuara coupling. (b) The enantioselective Rh-catalyzed Suzuki-Miyaura coupling to form Csp^3-Csp^2 bonds. (c) Application of this method to the synthesis of biologically active compounds.

We have developed a highly enantioselective Suzuki-type coupling between arylboronic acids and racemic cyclic allyl halides catalyzed by Rh-bisphosphine complexes (Fig. 1b).[11] We have demonstrated the use of vinyl and (hetero)arylboronic acids in combination with racemic (hetero)cyclic electrophiles.[12] The versatility of the method was highlighted by synthesis of the natural product (+)-isoananbasine,[12] and anticancer agent niraparib (Fig. 1c).[13] However, this transformation is currently limited to electrophiles that, after cleavage of the carbon–halogen bond, are achiral about the allyl unit.[13, 14]

In order to further understand the limitations and potential of Rh-catalysed asymmetric additions and of catalytic processes involving racemic substrates, we set out to design a series of experimental and computational experiments to reveal the mechanisms involved in this transformation.

Detailed mechanistic studies on Rh-catalyzed asymmetric additions are scarce. Hayashi and co-workers reported a key study on additions of arylboronic acids to cyclic α,β-unsaturated ketones.[15] For that transformation, after transmetalation, 2-cyclohexenone inserts into the Rh-aryl bond to form an oxa-π-allyl Rh species which hydrolyses to release the product. A subsequent kinetic study revealed that transmetalation from boron to Rh was the rate-determining step.[16]

Asymmetric allylic addition reactions with racemic electrophiles may occur *via* several distinct mechanistic

pathways, including those depicted in Fig. 2. Dynamic kinetic asymmetric transformations (DyKATs) catalyzed by Pd using stabilized nucleophiles occur *via* a well-understood mechanism; both enantiomers of the starting material are converted to a common pseudo-prochiral intermediate, and a subsequent outer-sphere addition of the nucleophile creates the new stereogenic centre.[17] A similar DyKAT mechanism may be operative here where oxidative addition (O.A.) of both enantiomers of the substrate results in a Rh-allyl species. Transmetalation of that species would be followed by an inner-sphere nucleophilic attack to give the arylated product (Fig. 2a).[18]

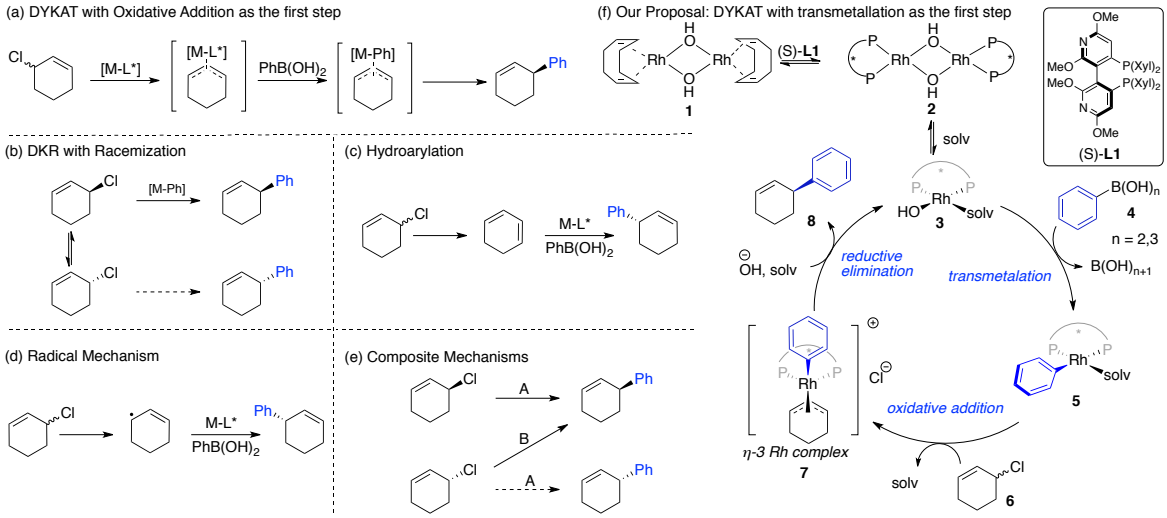

Figure 2. Plausible Mechanisms (a) DyKAT with O.A. as the first step (b) DKR with racemization of the starting material (c) Elimination to diene followed by hydroarylation (d) Mechanism with radical intermediate(s) (e) Composite mechanisms (f) The proposed mechanism in this work; DyKAT with transmetalation as the first step in the catalytic cycle.

Cu-catalyzed asymmetric addition of alkylzirconium reagents to racemic allylic substrates,[19] in contrast to Pd-catalyzed mechanisms, involves Dynamic Kinetic Resolution (DKR) facilitated by a Cu-halide-ligand complex.[20] The complex acts to interconvert enantiomers of the allyl chloride, as well as catalyze addition, and one enantiomer reacts more readily to give an enantioenriched product. The Rh-catalyzed arylation here could operate *via* a related mechanism, involving facile interconversion of substrate enantiomers followed by a stereospecific addition step (Fig. 2b).

Rh-catalysed hydroarlyation and Rh-catalysed processes involving diene electrophiles are known.[21-23] A mechanism could be operative here where elimination of the allyl halide forms a diene intermediate which then undergoes hydroarylation with a Rh-aryl species (Fig. 2c). Other plausible mechanisms, include various radical processes (Fig. 2d),[24 25] and direct enantioconvergent processes where the two starting enantiomers react *via* different mechanistic pathways to give the same enantiomer of the product (Fig. 2e).[26]

Here, we discuss a series of experimental and computational studies that rule out the mechanistic scenarios outlined above, and instead are fully consistent with the proposal shown in Fig. 2f. The available evidence is

congruent with the scenario in which a monomeric active catalytic species (**3**) reacts with the arylboronic acid (**4**) forming a Rh-aryl intermediate. Irreversible O.A. with both allyl chloride enantiomers yields a common η^3 complex (**7**), although one enantiomer of **6** reacts faster than the other. The subsequent reductive elimination (R.E.) step is enantiodetermining and sets the configuration of the product, as dictated by the absolute stereochemistry of the ligand.

Preliminary NMR Spectroscopic and Mechanistic Experiments

NMR spectroscopy was used to examine the reaction between $[Rh(cod)(OH)]_2$ and (*S*)-**L1** in THF-d_8. By comparing our data with literature reports,[15] we identified the formation of pre-catalytic species **2** (Figure 2f) and the mixed $[Rh_2(cod)(\mathbf{L1})(OH)_2]$ dimer (SI section 2.3). Rh-ligand dimer **2** undergoes rapid reaction with phenylboronic acid to give a Rh-aryl species. In contrast, when allyl chloride **6** was added to **2**, no reaction was observed even upon heating. These observations are not consistent with mechanisms initiated by the allylic electrophile first reacting with a metal-complex.[18]

Strikingly, formation of pre-catalyst **2** did not give a single clean species and was often accompanied by varying amounts of other species featuring ^{31}P singlet peaks at 25.7, 24.2 and –14.7 ppm, which we attribute to mono- and di-oxidized forms of ligand. Attempts to further characterize this reaction using *in situ* NMR spectroscopy were hindered by formation of complex mixtures of phosphorous containing species, which was not overcome by using alternative Rh complexes (see SI, section 2.4). Furthermore, when we attempted to follow reaction progress by *in situ* NMR spectroscopy, irreproducible results were obtained which we attribute to lack of stirring. Under these conditions some reaction components were found to be insoluble, complicating attempts to record meaningful kinetic data with the accuracy necessary to perform classical kinetic experiments. We therefore decided to probe the system using alternative experimental and computational techniques.

In related Cu-catalyzed transformations, we observed the interconversion of substrate enantiomers.[20] To examine if a similar process was occurring here, we used ^{1}H NMR exchange spectroscopy. However, under the reaction conditions, no exchange between vinylic and allylic protons in **6** was observed on the NMR timescale suggesting that the allyl chloride enantiomers don't interconvert *via* an S_N2' mechanism, or do so at a much slower rate than ^{1}H NMR relaxation. Therefore, a DKR mechanism (Fig. 2b) appears unlikely. This does not preclude racemization occurring during these reactions - it simply suggests that this is not a fundamental requirement of the reaction. A limitation of this experiment is that interconversion *via* S_N2 mechanisms cannot be detected.

To better understand the active catalytic species, we probed for nonlinear effects by measuring product (**8**) ee as a function of ligand (**L1**) ee.[27] A linear correlation between the enantiopurity of **L1** and **8** was observed, providing

no evidence for the involvement of high-order aggregates of the catalyst, consistent with an active catalytic species monomeric in Rh and **L1**. To test if the reaction could occur *via* the formation of an intermediate diene species (Fig. 2c), we used cyclohexa-1,3-diene in place of **6** but observed no arylated product. A reaction using d_5-phenylboronic acid showed the deuterium labels remained on the phenyl ring, ruling out mechanisms involving insertion of the Rh catalyst into C-H bonds of the aromatic ring.[22]

Competition Between Boronic Acids Nucleophiles

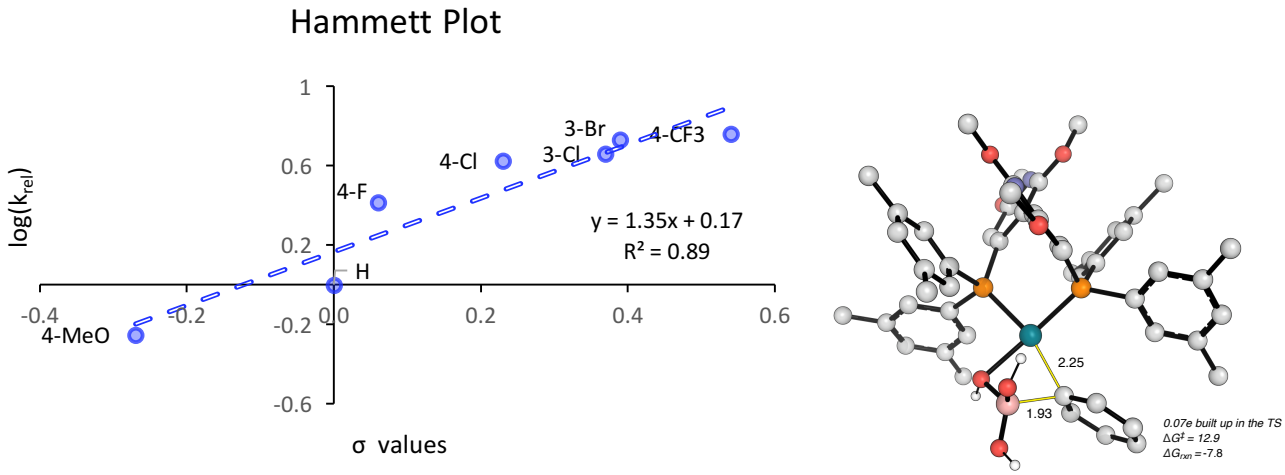

Figure 3. Hammett plot constructed from results of competition experiments between various meta- and para-substituted arylbonoric acids.

To probe the transmetalation step, we carried out a series of competition experiments using different arylboronic acids. There is a strong positive correlation between the ratio of products obtained and the Hammett substituent constants (σ values) of the arylboronic acids (Fig. 3).[28] This indicates transmetalation is faster with electron withdrawing substituents on the arylboronic acid, allowing electron deficient aryl species to preferentially and irreversibly enter the catalytic cycle, leading to formation of one product in excess. This preferential transmetallation could be due to increased Lewis acidity of the boron favouring formation of the boronate, and/or enhanced ability of electron poor substrates to stabilize partial negative charge during transmetallation.[29,30] The results with unsubstituted and MeO-substituted boronic acids deviate slightly from the trend, likely due to differing speciation. We believe that a role of the base in these reactions may be to aid in the formation of a boronate species. It is also likely that the base is required for active catalyst regeneration. Consistent with our experimental observations, the accumulation of negative charge in the aromatic ring was observed in the DFT-computed transition structure. Relative to the pre-transmetallation intermediate with a Rh-O-B linkage,[30,31] this elementary step is exergonic by 7.8 kcal/mol, consistent with irreversibility.

Natural abundance ^{13}C kinetic isotopic effects

We next focused our attention on the ensuing reaction between aryl-Rh species **5** and allyl chloride **6**, for which various possible mechanisms could be envisaged. To gain more understanding we sought to determine natural abundance $^{12}C/^{13}C$ ratios using the method developed by Singleton.[32,33] This approach has been employed with great success to measure competitive intermolecular ^{13}C kinetic isotope effects (KIE) in mechanistic studies of catalytic reactions.[34-42] This commonly relies on running the reaction to high conversion, and examining the $^{12}C/^{13}C$ ratio in recovered starting material. However, in the asymmetric addition to **6**, the isolation of small amounts of starting material at high conversions isn't possible as **6** is too sensitive to be reliably purified and may be configurationally labile during reaction or work-up conditions.[20] It is also plausible that the two enantiomers of **6** could undergo conversion at different rates, confounding analysis of KIE by examining the starting material. We therefore chose to determine $^{12}C/^{13}C$ ratios generated in product **8** when the reaction is quenched at low conversion and quantify the depletion of ^{13}C by quantitative ^{13}C NMR spectroscopy.

We performed the reactions on a 7.0 mmol scale as a relatively large amount of product is required for quantitative ^{13}C NMR spectroscopy and the reaction must be stopped at low conversion to ensure the product is enriched in the faster reacting isotope. However, using optimized conditions at this scale at 60 °C, the reaction was much faster than anticipated; when the reaction was quenched after 2 min, the conversion was already 60%. Suitable results could be obtained by stirring the reaction at 40 °C and quenching after 20 seconds. We repeated the process three times under these conditions, with experiments giving 10, 11 and 17% conversion (Fig. 3a). For the quantitative ^{13}C spectroscopy, we took C5 as the reference carbon. Although ^{13}C KIE are intrinsically small (ranging from 0.98–1.10),[43] after running these experiments in triplicate we observed appreciable KIE at positions C1, C3 and C7 (Fig. 4a).

For multi-step catalytic mechanisms, any observed isotope effects are the result of isotopic fractionation occurring at or before the first irreversible step that involves that reaction component.[44] Experimentally, we measured the largest KIE at C7 (1.027 ±0.006) and C3 (1.024 ±0.003), and a smaller, but still significant, KIE was obtained at C1 (1.010 ±0.005). As the transmetalation step is irreversible, ^{12}C fractionation at the aryl ipso-carbon (C7) of the product is most likely the result of a KIE in this elementary step.

To interpret the enrichment observed at C1 and C3, we calculated $^{12}C/^{13}C$ KIE that would result from various addition mechanisms (S_N2, S_N2'and reversible *anti*-O.A). The KIE values were calculated according to transition state theory applying the Bigeleisen–Mayer equation using scaled vibrational frequencies.[45,46] The calculated results for the most likely mechanism, as judged by comparing experimental and theoretical results, are shown in Fig. 4b-d (for other mechanisms see SI, Fig. S1).

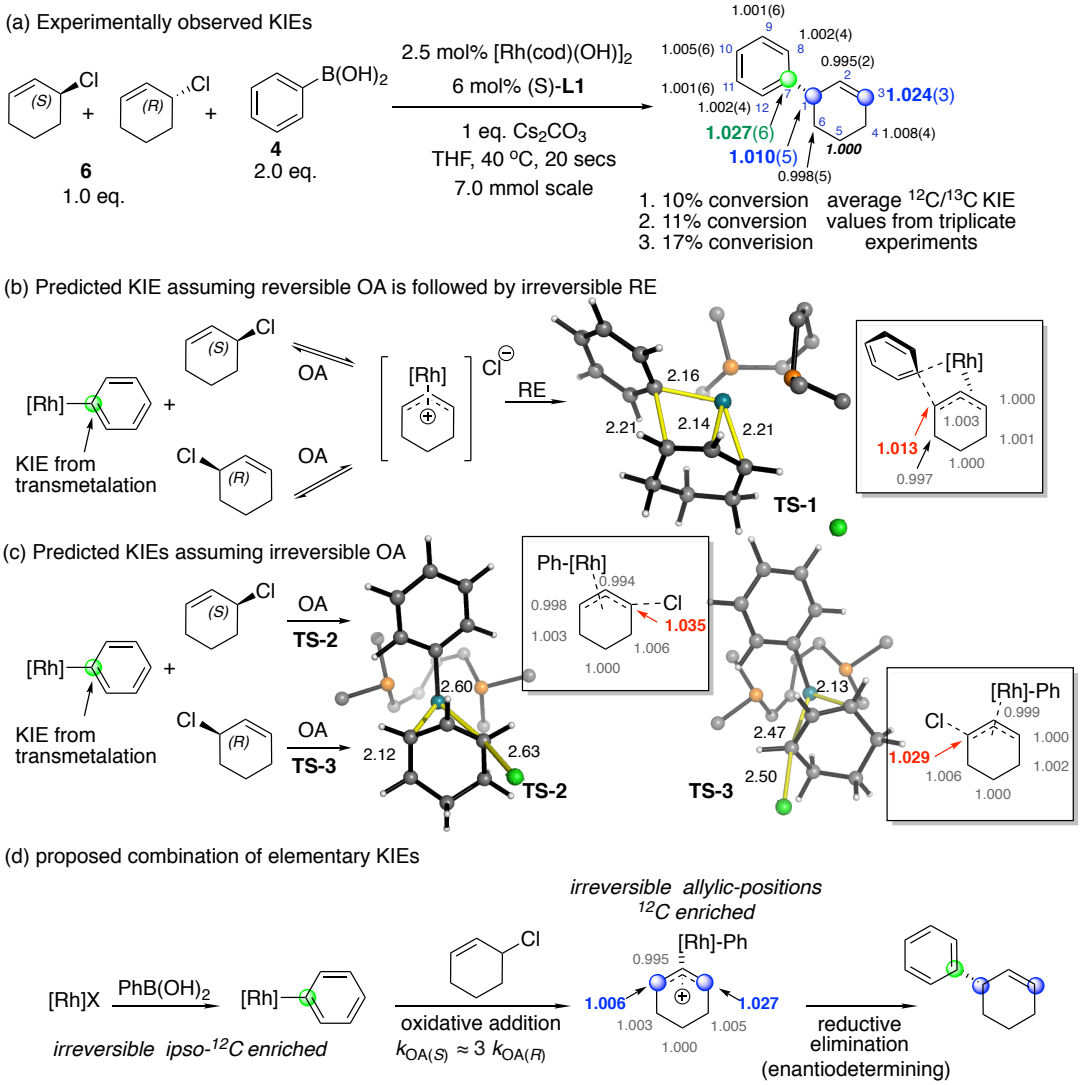

Figure 4. Examining the ^{13}C Kinetic Isotope Effect: (a) ^{13}C KIE experimental results, standard errors in parenthesis; (b) calculated ^{13}C KIE of stepwise mechanism with reversible *anti*-O.A. followed by irreversible R.E.; (c) calculated ^{13}C KIE of stepwise mechanism with irreversible *anti*-O.A.; (d) proposed combination of elementary KIE. A ratio of ~3.3:1 for OA of the *S* over the *R* enantiomer of the starting allyl chloride gives the observed level of ^{12}C enrichment. Computed TSs are shown with cropped ligands for clarity; selected distances are shown in Å.

In our proposed DyKAT mechanism with *anti*-O.A. followed by R.E., there are two plausible scenarios; one where O.A. is reversible and R.E. is the first irreversible step involving **6** (Fig. 4b), and another where O.A. is the first irreversible step in which **6** is involved (Fig. 4c). In the first scenario (Fig. 4b), the calculated KIE of C1 is 1.013 but there is no significant KIE at C3. The calculated KIE of only two carbons are within the experimental errors of the measured KIE. In the second scenario where O.A. is irreversible, the calculated KIE starting with (*S*)-**6** gave a value of 1.035 on C3, whereas with (*R*)-**6** gave KIE of 1.029 on C1 (Fig. 4c). If both enantiomers of **6** undergo an irreversible O.A., albeit at different rates, the observed KIE from product analysis will be a weighted average from both starting enantiomers. From our calculations, a 3.3:1 ratio of (*S*)- to (*R*)-**6** undergoing O.A. accounts quantitatively for the experimentally observed KIE on all six carbons of the allyl unit (Fig. 4d).

These experiments are inconsistent with other possible mechanisms for the Rh-catalyzed process, including radical and composite mechanisms (Fig. 2d and e). Overall the ^{13}C KIE support a mechanism where the first step in the catalytic cycle is an irreversible transmetalation, followed by an irreversible *anti*-O.A. where the enantiomers of **6** react at different rates.

DFT calculations

DFT calculations[47] were performed using the ωB97X-D functional.[48] In geometry optimizations, LANL2DZ(f) (orbital exponent of 1.35) effective core potential (ECP)/valence double-ζ basis set was used for Rh and the split-valence 6-31G(d) basis set was used for other atoms. Single point energy corrections were obtained with an implicit description of the reaction medium by SMD solvent model at the ωB97X-D/6-311+G(d,p) level of theory with the LANL2TZ(f) ECP/valence triple-ζ basis set for Rh. The Gibbs energy profile for transmetalation, oxidative addition and reductive elimination steps are illustrated in Fig. 5. Other possible mechanisms were also calculated but found to have higher reaction barriers (see SI, Fig. S1).

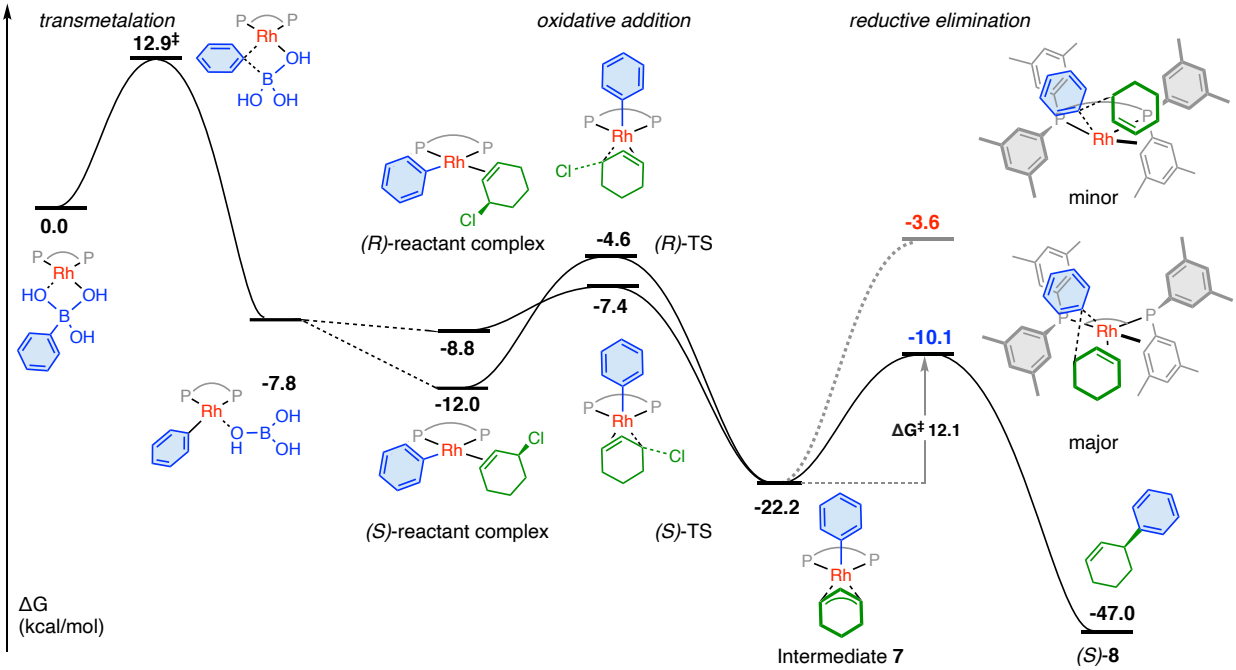

Figure 5. A condensed Gibbs energy profile of O.A. followed by R.E. (SMD(THF)-ωB97X-D/6-311+G(d,p), LANL2TZ(f) // ωB97X-D/6-31G(d), LANL2DZ(f)).

Calculations suggest that the key process for enabling the use of racemic **6** in this DyKAT is O.A. to give a common η-3 intermediate where the stereochemical information of **6** is lost. The energy barrier of O.A. for (*R*)-**6** is calculated to be higher than (*S*)-**6**, in qualitative agreement with natural abundance ^{13}C KIE experiments. Subsequently, the intermediate undergoes R.E. wherein the stereochemistry of the product is set due the spatial constraints the C_2-

symmetric ligand imposes on the allyl unit and the phenyl group. From these calculations we deduce that R.E. is enantiodetermining, as the new stereogenic center is predicted to form irreversibly in this step.[49] The large calculated difference in energy between the R.E. TSs ($\Delta\Delta E^{\ddagger}$ = 5.5 kcal/mol, $\Delta\Delta G^{\ddagger}$ = 7.2 kcal/mol) is consistent with both the sense and very high levels of enantioselectivity observed experimentally for the formation of (*S*)-**8** in >99% ee. Transmetalation and oxidative addition steps are both predicted to take place irreversibly. The consequence of an irreversible oxidative addition is that the diastereoselectivity is determined in this step.

Arylation with Heterocyclic and Other Allyl Chlorides

We also calculated the energy profile for the pyranyl substrate **9** and found that the reaction barrier is much lower than that of **6** (see SI, Fig. S2). A competition experiment between allyl chlorides **6** and **9** was performed (Fig. 6a). After 1 hour, the product ratio was 20:1 in favour of product **10**, indicating that O.A. is faster for **9** which is qualitatively in agreement with the results of our DFT calculations.

Both ^{13}C KIE experiments and DFT calculations suggests that there are differences in the rate of O.A. of the enantiomers of (±)-**6**. Based on this hypothesis, an increase in ee of **6** over the course of the reaction would be anticipated. Despite several attempts, any ee of **6** couldn't be reliably measured and enantiopure **6** likely cannot be obtained due to its high reactivity,[20] precluding us from directly probing the relative rate of O.A. of the enantiomers of **6**. However, this could be probed using piperidinyl allyl chloride **11** which was found to be configurationally stable.[50]

We monitored the ee of **11** under the conditions used in the ^{13}C KIE measurements and found that the ee of **11** increases from 0 to 94% ee over 1 hour (Fig. 6b), supporting the idea that the rate of O.A. differs for the two enantiomers of the substrate. This also supports our earlier conclusion that fast interconversion of substrate enantiomers is not required for this asymmetric reaction.

Interestingly, under alternative conditions, previously optimized for **11**, using (*S*)-**L2**, enantioenrichment of **11** was not observed (Fig. 6d). This observation was unchanged at a 30 ºC, and so the resolution of starting materials is likely a ligand effect. These ligands impose different steric environments on the O.A. TSs therefore leading to different relative energies between the O.A. TSs of the two enantiomers of the allyl chloride. Under the conditions shown in fig. 6d, both enantiomers of **11** may react at comparable rates due to reduced steric constraints in the O.A. TSs.

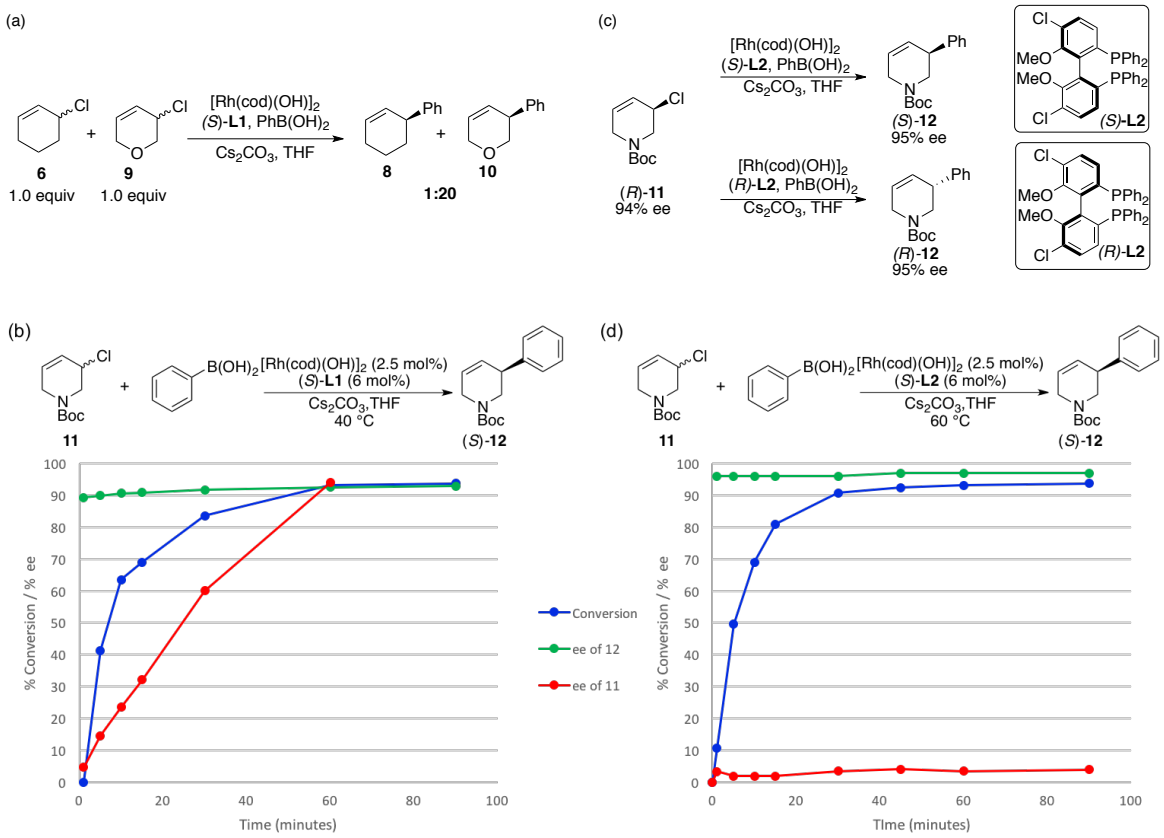

Figure 6. (a) Competition experiment with allyl chlorides (±)-**6** and (±)-**13**. (2.5 mol % $[Rh(cod)(OH)]_2$, 6 mol % **L1**, 1 equiv. of $PhB(OH)_2$). (b) Measuring the ee over the course of the reaction with allyl chloride **11** using **L1**. (c) Arylation of enantioenriched (+)-**11** with both enantiomers of **L2**. (2.5 mol % $[Rh(cod)(OH)]_2$, 6 mol % **L2**, 2 equiv. of $PhB(OH)_2$) (d) Measuring the ee over the course of the reaction with allyl chloride **11** using **L2**.

In both of these experiments, we observed that the ee of **12** is constant as a function of time, supporting the idea that R.E. is the stereodetermining step.

We were able to access enantioenriched (*R*)-**11**,[50] and subjected (*R*)-**11** (94% ee) to reaction conditions with each enantiomer of **L2** (Fig. 6c). With (*S*)-**L2**, we obtained (*S*)-**12** (95% ee), whereas with (*R*)-**L2**, the other enantiomer of the product ((*R*)-**12,** –95% ee) was obtained. Therefore, the absolute stereochemistry of the product is determined by the stereochemistry of the ligand and isn't affected by the stereochemistry of the allyl chloride. Interestingly, with (*R*)-**L2**, the reaction was considerably slower and we observed deterioration of the ee of (*R*)-**11** (94% to 82% ee over 6 hours), suggesting that racemization may occur slowly but it isn't essential for product formation.

Isotopically labelled **11**-*d* was synthesized with a deuterium atom at the vinylic position.[50] Under the conditions shown in Fig. 7a, addition to (±)-**11**-C3-*d* gave a 1:1 ratio of products with deuterium at C3 and C5. Due to the ^{2}H-label at the vinylic position in each enantiomer of starting material, the two enantiomers can no longer form a

common intermediate after O.A.. One enantiomer reacts to give one intermediate which, after R.E., leads to one pseudo-regioisomer of the product and the other reacts to give the alternative pseudo-regioisomer.

Therefore, if O.A. is faster with one enantiomer of **11**, and enantioenriched ^{2}H-labelled **11** is used, the products should have an excess of the deuterium label at one position (allylic or vinylic) depending on the stereochemistry of the ligand used. After subjecting (*R*)-**11**-C3-*d* (94% ee) to optimized reaction conditions with (*S*)-**L2**, the majority of deuterium remained at C3 in product (*S*)-**12**, whereas with (*R*)-**L2**, the majority of deuterium was found at the allylic position of (*R*)-**12** (Fig. 7b).

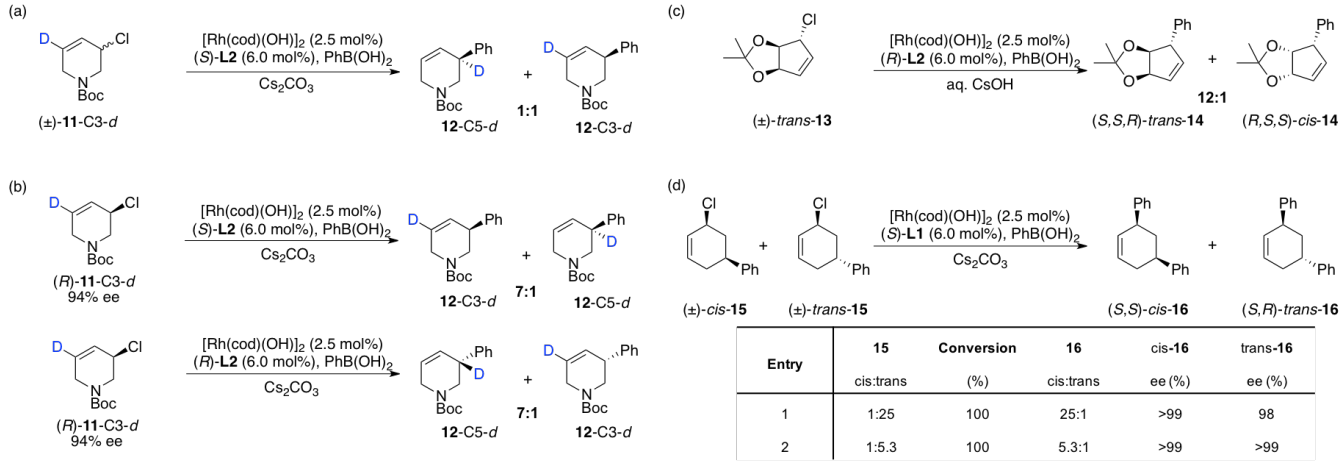

Entry	15 cis:trans	Conversion (%)	16 cis:trans	cis-16 ee (%)	trans-16 ee (%)
1	1:25	100	25:1	>99	98
2	1:5.3	100	5.3:1	>99	>99

Figure 7. Asymmetric allylic arylation with heterocyclic and other allyl chlorides. All reactions were done in THF at 60 °C. (a) Arylation of (±)-*d*-**11**. (b) Arylation of (*R*)-*d*-**11** with both enantiomers of **L2**. (c) Arylation of bicyclic substrates showing evidence for *syn*-O.A. (d) Arylation of diastereomeric 5-phenyl substituted starting materials showing evidence for *anti*-O.A.

According to our proposed mechanism of *anti*-O.A., we expected ((*R*)-**11**-C3-*d*) to give the opposite results obtained in terms of observed pseudo-regioisomer preference with each enantiomer of the ligand. Our experimental results surprisingly indicate that with **11**, *syn*-O.A. is the major pathway. In each case, there is a small percentage of deuterium scrambling (7:1 ratio) which we attribute to a 7:1 ratio of *syn* and *anti* O.A. steps occurring. At this stage we cannot rule of that the scrambling is due to slow racemization of **11** over the course of the reaction, or alternatively isomerization after O.A. *via* nucleophilic displacement with Rh(I) species in analogy to mechanistic pathways observed in Pd(0)-catalysis.[51]

Recently, we discovered that the related Rh-catalyzed enantioselective additions to fused bicyclic substrates give stereochemical results consistent with *syn*-selective addition to racemic allyl chloride starting materials (Fig. 7c).[14] To further probe these experimental results, we compared the *syn*- and *anti*- transition states arising from O.A. to **13** using DFT calculations (Fig. 8). The results show that steric clash between the substrates acetal bridge and

ligand used is key to determining the facial selectivity of O.A.. It is important to note here that O.A. is the diastereodetermining step in this system, while R.E. remains in control of the absolute stereochemistry.

DFT calculations for model substrate **6** (Fig. 5 and 8) clearly indicate that in **6** *anti*-O.A. is favoured. We have also examined enantioselective additions to phenyl-substituted allyl chlorides,[11] where mixtures of the four stereoisomers of 3-chloro-5-phenylcyclohex-1-ene (**15**) gave overall enantioselective inversion to *cis*- and *trans*-**16** (Fig. 7d). These experiments, where we observe highly enantioselective overall inversion to form *cis*- and *trans*-**16**, are consistent with *anti*-O.A. with an aryl-Rh species, followed by inner-sphere attack of the aryl nucleophile, delivering the phenyl on the same side of the allyl ion as the Rh.

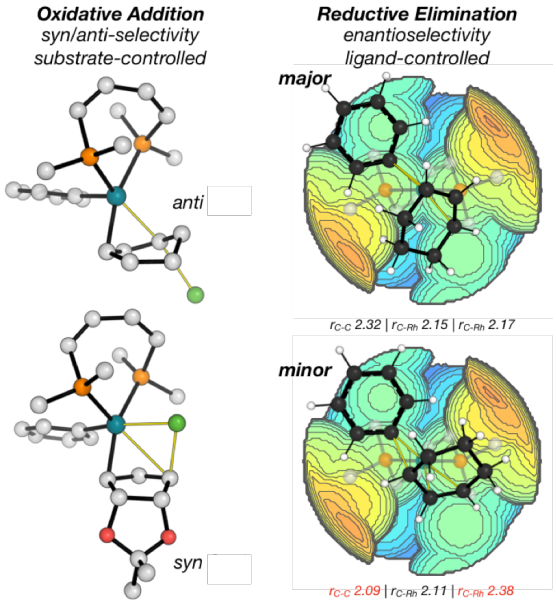

Figure 8. Simplified models showing the origins of diastereoselectivity and enantioselectivity in this Rh(I)-Catalyzed Asymmetric Suzuki Miyaura Coupling. Favoured *anti*-O.A. TS for **6** and favoured *syn*-O.A. TS for **13** shown. Catalytic pocket images generated using: SambVca 2.1.[52]

Therefore, we have experimentally observed and computationally validated that Rh species can add to allyl halide substrates *via syn*- or *anti*-O.A., depending on the steric accessibility of the substrate (Fig. 8). The oxidative addition step dictates diastereoselectivity and is influenced by the substrate, while the overall sense of enantioselectivity is catalyst-controlled and set in the reductive elimination step. The high enantioselectivity observed experimentally is reflected in the large difference in energy between the reductive elimination transition states. This can be attributed to steric effects between the ligand and allyl fragment, which in turn give rise to substantial differences in key bond distances between the two competing TSs. An analysis of the catalytic pocket (Fig. 8) emphasises the narrow groove provided by the ligand in which the reductive elimination must take place.[52] The minor TS structure has

weaker coordination between alkene and Rh, and a much shorter forming C-C bond (i.e. a later TS) – compared to the favoured structure, which is consistent with the large energy difference between the two.

Conclusion

The asymmetric Suzuki-Miyaura coupling of arylboronic acids with racemic allylic halides catalyzed by a Rh(I) complex gives highly enantioenriched arylated products. We have used a variety of techniques to elucidate a mechanistic proposal. Here the active catalytic species is monomeric in Rh and ligand and irreversible transmetalation between boron and Rh is the first step in the catalytic cycle. Experimentally observed natural abundance ^{13}C KIEs in combination with theoretical calculations were key to demonstrating that O.A. occurs in a ~3.3:1 ratio in favour of one enantiomer over the other. A common pseudo-symmetrical η^3 Rh-allyl complex is formed by irreversible O.A. of Rh-aryl intermediates to both enantiomers of the racemic substrates. Interestingly, O.A. can occur in a *syn*- or *anti*- fashion depending on the steric accessibility of the substrate. The symmetry of η^3 Rh-allyl complexes formed by O.A. was probed using configurationally stable, racemic and enantiomerically enriched, and deuterium labelled piperidinyl allyl chlorides along with racemic diastereomeric substituted allyl chlorides. These studies support the proposed promiscuity of the O.A. step and demonstrate that R.E. of common intermediates formed from both enantiomers give highly enantioenriched products where the diastereoselectivity is determined by O.A. and absolute stereochemistry of the product is dictated by the ligand. We foresee that this study will contribute to the broader understanding of asymmetric Rh-allyl chemistry and will enable the discovery, exploitation and understanding of new asymmetric reactions with racemic substrates.

Data Availability Statement Experimental details and analytical data for all experiments, absolute energies and selected distances for all DFT computed structures and cartesian coordinates (in xyz format) for computed stationary points can be found in the supporting information.

Code Availability Statement All Python scripts used for data analysis have been made available - https://github.com/bobbypaton - under a creative commons CC-BY license.

Acknowledgments The EPSRC supports this work though standard grant EP/N022246/1. L.v.D. and R.A. are grateful to the EPSRC Centre for Doctoral Training (CDT) in Synthesis for Biology and Medicine (EP/L015838/1) for studentships, generously supported by AstraZeneca, Diamond Light Source, Defence Science and Technology Laboratory, Evotec, GlaxoSmithKline, Janssen, Novartis, Pfizer, Syngenta, Takeda, UCB and Vertex. R.A. also

acknowledges the Development and Promotion of Science and Technology Talents Project and the Royal Thai Government. We used the Dirac cluster at Oxford supported by the EPSRC CDT for Theory and Modelling in Chemical Sciences (EP/L015722/1), the RMACC Summit supercomputer, which is supported by the National Science Foundation (ACI-1532235 and ACI-1532236), the University of Colorado Boulder and Colorado State University, and the Extreme Science and Engineering Discovery Environment (XSEDE) through allocation TG-CHE180056 and computing resources provided by the National e-Science Infrastructure Consortium, Thailand. O.S. thanks the Scientific and Technological Research Council of Turkey for the 2214-A Scholarship Programme.

Author Contributions S.P.F. conceived and directed the project. S.P.F., L.v.D and M.S. designed the experiments. L.v.D., M.S. and S.K. performed the experiments. L.v.D., R.A., M.S., S.K., R.P. and S.P.F. analyzed the experimental results. R.S.P, L.v.D, R.A. and O.S. designed, conducted and analyzed the computational work. T.D.W.C. designed and performed the ^{13}C NMR experiments. S.P.F., R.S.P, T.D.W.C., L.v.D, M.S. and R.A. were involved in manuscript preparation.

Keywords: Asymmetric Catalysis • Density Functional Calculations • Isotope Effects • Reaction Mechanisms • Rhodium

(1) Hall, D. G. Boronic Acids: Preparation and Applications in Organic Synthesis and Medicine; Wiley-VCH, Weinheim, **2006**.

(2) Suzuki, A. Cross-Coupling Reactions of Organoboranes: An Easy Way To Construct C-C Bonds (Nobel Lecture). *Angew. Chem. Int. Ed.* **2011**, *50*, 6722–6737.

(3) Cherney, A. H.; Kadunce, N. T.; Reisman, S. E. Enantioselective and Enantiospecific Transition-Metal-Catalyzed Cross-Coupling Reactions of Organometallic Reagents to Construct C-C Bonds. *Chem. Rev.* **2015**, *115*, 9587–9652.

(4) Dong, L.; Xu, Y. J.; Cun, L. F.; Cui, X.; Mi, A. Q.; Jiang, Y. Z.; Gong, L. Z. Asymmetric Nitroallylation of Arylboronic Acids with Nitroallyl Acetates Catalyzed by Chiral Rhodium Complexes and Its Application in a Concise Total Synthesis of Optically Pure (+)-γ-Lycorane. *Org. Lett.* **2005**, *7*, 4285–4288.

(5) Yu, B.; Menard, F.; Isono, N.; Lautens, M. Synthesis of Homoallylic Alcohols via Lewis Acid Assisted Enantioselective Desymmetrization. *Synthesis (Stuttg).* **2009**, 853–859.

(6) Shintani, R.; Takatsu, K.; Takeda, M.; Hayashi, T. Copper-Catalyzed Asymmetric Allylic Substitution of Allyl Phosphates with Aryl- and Alkenylboronates. *Angew. Chem. Int. Ed.* **2011**, *50*, 8656–8659.

(7) Zhang, P.; Brozek, L. A.; Morken, J. P. Pd-Catalyzed Enantioselective Allyl-Allyl Cross-Coupling. *J. Am. Chem. Soc.* **2010**, *132*, 10686–10688.

(8) Chung, K.; Miyake, Y.; Uemura, S. Nickel(0)-Catalyzed Asymmetric Cross-Coupling Reactions of Allylic Compounds with Grignard Reagents Using Optically Active Oxazolinylferrocenylphosphines as Ligands. *J. Chem. Soc*., *Perkin Trans. 1* **2000**, 2725–2729.

(9) Ohmiya, H.; Makida, Y.; Tanaka, T.; Sawamura, M. Palladium-Catalyzed γ-Selective and Stereospecific Allyl−Aryl Coupling between Allylic Acetates and Arylboronic Acids. *J. Am. Chem. Soc.* **2008**, *130*, 17276–17277.

(10) Ohmiya, H.; Yokokawa, N.; Sawamura, M. Copper-Catalyzed Gamma-Selective and Stereospecific Allyl-Aryl Coupling between (Z)-Acyclic and Cyclic Allylic Phosphates and Arylboronates. *Org. Lett.* **2010**, *12*, 2438–2440.

(11) Sidera, M.; Fletcher, S. P. Rhodium-Catalyzed Asymmetric Allylic Arylation of Racemic Halides with Arylboronic Acids. *Nat. Chem.* **2015**, *7*, 935–939.

(12) Schäfer, P.; Palacin, T.; Sidera, M.; Fletcher, S. P. Asymmetric Suzuki-Miyaura Coupling of Heterocycles via Rhodium-Catalyzed Allylic Arylation of Racemates. *Nat. Commun.* **2017**, *8*, 15762–15769.

(13) González, J.; van Dijk, L.; Goetzke, F.W.; Fletcher, S. P. Highly enantioselective Rhodium-Catalyzed Cross-Coupling of Boronic Acids and Racemic Allyl Halides. *Nat Protoc*, **2019**, *14***,** 2972–2985.

(14) Goetzke, F. W.; Mortimore, M.; Fletcher, S. P. Enantio- and Diastereoselective Suzuki‐Miyaura Coupling with Racemic Bicycles. *Angew. Chem. Int. Ed.* **2019**, *58*, 12128–12132.

(15) Hayashi, T.; Takahashi, M.; Takaya, Y.; Ogasawara, M. Catalytic Cycle of Rhodium-Catalyzed Asymmetric 1, 4-Addition of Organoboronic Acids. Arylrhodium, Oxa-π-Allylrhodium, and Hydroxorhodium Intermediates. *J. Am. Chem. Soc.* **2002**, *124*, 5052–5058.

(16) Kina, A.; Iwamura, H.; Hayashi, T. A Kinetic Study on Rh/Binap-Catalyzed 1,4-Addition of Phenylboronic Acid to Enones: Negative Nonlinear Effect Caused by Predominant Homochiral Dimer Contribution. *J. Am. Chem. Soc.* **2006**, *128*, 3904–3905.

(17) Pfaltz, A.; Lautens, M.; Jacobsen, E. N.; Pfaltz, A.; Yamamoto, H. *Comprehensive Asymmetric Catalysis II* **1999**.

(18) Turnbull, B. W. H.; Evans, P. A. Asymmetric Rhodium-Catalyzed Allylic Substitution Reactions: Discovery, Development and Applications to Target-Directed Synthesis. *J. Org. Chem.* **2018**, *83*, 11463–11479.

(19) You, H.; Rideau, E.; Sidera, M.; Fletcher, S. P. Non-Stabilized Nucleophiles in Cu-Catalyzed Dynamic Kinetic Asymmetric Allylic Alkylation. *Nature* **2015**, *517*, 351–355.

(20) Rideau, E.; You, H.; Sidera, M.; Claridge, T. D. W.; Fletcher, S. P. Mechanistic Studies on a Cu-Catalyzed Asymmetric Allylic Alkylation with Cyclic Racemic Starting Materials. *J. Am. Chem. Soc.* **2017**, *139*, 5614–5624.

(21) Tsui, G. C.; Menard, F.; Lautens, M.; Regioselective Rhodium(I)-Catalyzed Hydroarylation of Protected Allylic Amines with Arylboronic Acids. *Org. Lett.*, **2010**, *12*, 2456–2459.

(22) Yang, Q.; Wang, Y.; Luo, S.; Wang, J.; Kinetic Resolution and Dynamic Kinetic Resolution of Chromene by Rhodium-Catalyzed Asymmetric Hydroarylation. *Angew. Chem. Int. Ed*. **2019**, *58*, 5343 –5347.

(23) Yang, X.; Davison, R. T.; Nie, S.; Cruz, F. A.; McGinnis, T. M.; Dong, V. M.; Catalytic Hydrothiolation: Counterion-Controlled Regioselectivity. *J. Am. Chem. Soc.* **2019**, *141*, 3006−3013.

(24) Lu, Z.; Wilsily, A.; Fu, G. C.; Stereoconvergent Amine-Directed Alkyl-Alkyl Suzuki Reactions of Unactivated Secondary Alkyl Chlorides. *J. Am. Chem. Soc.* **2011**, *133*, 8154–8157.

(25) Gutierrez, O.; Tellis, J. C.; Primer, D. N.; Molander, G. A.; Kozlowski, M. C.; Nickel-Catalyzed Cross-Coupling of Photoredox-Generated Radicals: Uncovering a General Manifold for Stereoconvergence in NickelCatalyzed Cross-Couplings. *J. Am. Chem. Soc.* **2015**, *137*, 4896−4899.

(26) Langlois, J.; Emery, D.; Mareda, J.; Alexakis, A.; Mechanistic identification and improvement of a direct enantioconvergent transformation in copper-catalyzed asymmetric allylic alkylation. *Chem. Sci.*, **2012**, *3*, 1062−1069.

(27) Girard, C.; Kagan, H. B. Nonlinear Effects in Asymmetric Synthesis and Stereoselective Reactions: Ten Years of Investigation. *Angew. Chem. Int. Ed.* **1998**, *37*, 2922–2959.

(28) Mc Daniel, D. H.; Brown, H. C. An Extended Table of Hammett Substituent Constants Based on the Ionization of Substituted Benzoic Acids. *J. Org. Chem.* **1958**, *23*, 420–427.

(29) Lennox, A. J. J.; Lloyd-Jones, G. C.; Transmetalation in the Suzuki–Miyaura Coupling: The Fork in the Trail. *Angew. Chem. Int. Ed.* **2013**, *52*, 7362–7370.

(30) Thomas, A. A.; Denmark, S. E.; Pre-transmetalation intermediates in the Suzuki-Miyaura reaction revealed: The missing link. *Science*, **2016**, *352*, 329–332.

(31) Yaman, T.; Harvey, J. N.; Suzuki–Miyaura coupling revisited: an integrated computational study. *Faraday Discuss.*, **2019**, *220*, 425-442.

(32) Singleton, D. A.; Thomas, A. A. High-Precision Simultaneous Determination of Multiple Small Kinetic Isotope Effects at Natural Abundance. *J. Am. Chem. Soc.* **1995**, *117*, 9357–9358.

(33) Frantz, D. E.; Singleton, D. A.; Snyder, J. P. 13 C Kinetic Isotope Effects for the Addition of Lithium Dibutylcuprate to Cyclohexenone. Reductive Elimination Is Rate-Determining. *J. Am. Chem. Soc.* **1997**, *119*, 3383–3384.

(34) Li, J.; Huang, R.; Xing, Y. K.; Qiu, G.; Tao, H. Y.; Wang, C.J. Catalytic Asymmetric Cascade Vinylogous Mukaiyama 1,6-Michael/Michael Addition of 2-Silyloxyfurans with Azoalkenes: Direct Approach to Fused Butyrolactones. *J. Am. Chem. Soc.* **2015**, *137*, 10124–10127.

(35) Colletto, C.; Islam, S.; Juliá-Hernández, F.; Larrosa, I. Room-Temperature Direct β-Arylation of Thiophenes and Benzo[*b*]Thiophenes and Kinetic Evidence for a Heck-Type Pathway. *J. Am. Chem. Soc.* **2016**, *138*, 1677–1683.

(36) Smith, J. R.; Collins, B. S. L.; Hesse, M. J.; Graham, M. A.; Myers, E. L.; Aggarwal, V. K. Enantioselective Rhodium(III)-Catalyzed Markovnikov Hydroboration of Unactivated Terminal Alkenes. *J. Am. Chem. Soc.* **2017**, *139*, 9148–9151.

(37) Rathbun, C. M.; Johnson, J. B. Rhodium-Catalyzed Acylation with Quinolinyl Ketones: Carbon−Carbon Single Bond Activation as the Turnover-Limiting Step of Catalysis. *J. Am. Chem. Soc.* **2011**, *133*, 2031–2033.

(38) Moore, J. L.; Silvestri, A. P.; de Alaniz, J. R.; DiRocco, D. A.; Rovis, T. Mechanistic Investigation of the Enantioselective Intramolecular Stetter Reaction: Proton Transfer Is the First Irreversible Step. *Org. Lett.* **2011**, *13*, 1742–1745.

(39) Lee, D. H.; Kwon, K. H.; Yi, C. S. Selective Catalytic C-H Alkylation of Alkenes with Alcohols. *Science* **2011**, *333*, 1613–1616.

(40) Meyer, M. P. New Applications of Isotope Effects in the Determination of Organic Reaction Mechanisms; Elsevier, **2012**.

(41) Vo, L. K.; Singleton, D. A. Isotope Effects and the Nature of Stereo- and Regioselectivity in Hydroaminations of Vinylarenes Catalyzed by Palladium(II)−Diphosphine Complexes. *Org. Lett.* **2004**, *6*, 2469–2472.

(42) Roytman, V. A.; Karugu R. W.; Hong, Y.; Hirschi, J. S.; Vetticatt, M. J.; ^{13}C Kinetic Isotope Effects as a Quantitative Probe To Distinguish between Enol and Enamine Mechanisms in Aminocatalysis. *Chem. Eur. J.* **2018**, *24*, 8098 –8102.

(43) Wolfsberg, M.; Van Hook, W. A.; Paneth, P.; Rebelo, L. P. N. Isotope Effects in the Chemical, Geological, and Bio Sciences; Springer, Dordrecht, **2010**.

(44) Simmons, E. M.; Hartwig, J. F. On the Interpretation of Deuterium Kinetic Isotope Effects in C-H Bond Functionalizations by Transition-Metal Complexes. *Angew. Chem. Int. Ed.* **2012**, *51*, 3066–3072.

(45) Deb, A.; Hazra, A.; Peng, Q.; Paton, R. S.; Maiti, D.; Detailed Mechanistic Studies on Palladium-Catalyzed Selective C−H Olefination with Aliphatic Alkenes - A Significant Influence of Proton Shuttling. *J. Am. Chem. Soc.* **2017**, *139*, 763–775.

(46) Mekareeya, A.; Walker, P. R.; Couce-Rios, A.; Campbell, C. D.; Steven, A.; Paton, R. S.; Anderson, E. A. Mechanistic insight into palladium-catalyzed cycloisomerization: A combined experimental and theoretical study. *J. Am. Chem. Soc.* **2017**, *139*, 10104–10114.

(47) Gaussian 09, Revision D.01, M. J. Frisch, G. W. Trucks, H. B. Schlegel, G. E. Scuseria, M. A. Robb, J. R. Cheeseman, G. Scalmani, V. Barone, B. Mennucci, G. A. Petersson, H. Nakatsuji, M. Caricato, X. Li, H. P. Hratchian, A. F. Izmaylov, J. Bloino, G. Zheng, J. L. Sonnenberg, M. Hada, M. Ehara, K. Toyota, R. Fukuda, J. Hasegawa, M. Ishida, T. Nakajima, Y. Honda, O. Kitao, H. Nakai, T. Vreven, J. A. Montgomery, Jr., J. E. Peralta, F. Ogliaro, M. Bearpark, J. J. Heyd, E. Brothers, K. N. Kudin, V. N. Staroverov, R. Kobayashi, J. Normand, K. Raghavachari, A. Rendell, J. C. Burant, S. S. Iyengar, J. Tomasi, M. Cossi, N. Rega, J. M. Millam, M. Klene, J. E. Knox, J.

B. Cross, V. Bakken, C. Adamo, J. Jaramillo, R. Gomperts, R. E. Stratmann, O. Yazyev, A. J. Austin, R. Cammi, C. Pomelli, J. W. Ochterski, R. L. Martin, K. Morokuma, V. G. Zakrzewski, G. A. Voth, P. Salvador, J. J. Dannenberg, S. Dapprich, A. D. Daniels, Ö. Farkas, J. B. Foresman, J. V. Ortiz, J. Cioslowski, and D. J. Fox, Gaussian, Inc., Wallingford CT, **2009**.

(48) Straker, R.; Peng, Q.; Mekareeya, A.; Paton, R. S.; Anderson, E. A. Computational Ligand Design in Enantio- and Diastereoselective Ynamide [5+2] Cycloisomerizations. *Nature Commun.* **2015**, *7*, 10109–10118.

(49) Peng, Q.; Duarte, F.; Paton, R. S.; Computing Organic Stereoselectivity – from Concepts to Quantitative Calculations and Predictions. *Chem. Soc. Rev.* **2016**, *45*, 6093–6107.

(50) Karabiyikoglu, S.; Brethomé, A.; Palacin, T.; Paton, R. S.; Fletcher, S. P. Allylic Chloro-Tetrahydropyridines: Kinetic Resolutions and Stereospecific Reactions of Enantiomerically Enriched Allyl Chlorides. *ChemRxiv. Preprint*. **2019**, doi:10.26434/chemrxiv.8181686.v.

(51) Granberg, K. L.; Bäckvall, J. E.; Isomerization of (π-Allyl)palladium Complexes *via* Nucleophilic Displacement by Palladium(0). A Common Mechanism in Palladium(0)-Catalyzed Allylic Substitution. *J. Am. Chem. Soc.* **1992**, *114*, 6858–6863.

(52) Falivene, L.; Cao, Z.; Petta, A.; Serra, L.; Poater, A.; Oliva, R.; Scarano, V.; Cavallo, L. Towards the Online Computer-Aided Design of Catalytic Pockets. *Nat. Chem.* **2019**, *11*, 872–879.